Cell Motility 1:205–235 (1981)

# Motion of Polymorphonuclear Leukocytes: Theory of Receptor Redistribution and the Frictional Force on a Moving Cell

**Micah Dembo, Laurette Tuckerman, and Walter Goad**

*Theoretical Division, Los Alamos Scientific Laboratory, University of California, Los Alamos, New Mexico*

As a cell moves over a surface, the distribution of membrane proteins that adhere to the surface will be changed relative to the distribution of these molecules on a static cell. Observations of this redistribution offer, in principle, evidence as to the mechanisms of membrane dynamics during cell locomotion. Toward extracting such information we present and analyze a mathematical model of receptor transport in the membrane by diffusion and convection, as affected by the making and breaking of the bonds between the receptors and the surface as the cell moves.

We show that the disruption of receptor-surface bonds at the tail of the cell provides a mechanism by which the frictional force opposing a cell's motion is exerted, and calculate the magnitude of this force as a function of cell velocity. Assuming this to be the major contribution to the frictional force, we show that when the shear force on a cell is above a critical value it is no longer possible for the cell to slide across the surface. For such large forces, it is still possible for the cell to roll; alternatively the cell can be torn free of the surface.

Our analysis of existing data on movement of polymorphonuclear leukocytes indicates that cell motion is not accompanied by a bulk flow of membrane from the front to the back of the cell. The data also indicate that cells do not tend to roll as they move over a surface under normal conditions. The data are most consistent with a model where the membrane as a whole is stationary but where receptors that bind to the surface become coupled to submembrane contractile proteins.

**Key words: capping of receptors, cell locomotion, cell-surface interactions, frictional force, membrane flow, polymorphonuclear leukocytes**

## INTRODUCTION

Locomotion of polymorphonuclear leukocytes (PMNs) (also called granulocytes) is associated with formation of a tapered process or tail at the posterior end of the cell which we will call the uropod [Robineaux, 1954; Greenwood, 1969; Ramsey, 1972b; Armstrong and Lackie, 1975; Stossel, 1977]. Observers frequently remark that the uropod gives the impression of close attachment to the substratum [Armstrong and Lackie, 1975; Stossel, 1977; King et al, 1980]. This impression is reinforced by the observations that, as the cell

Address reprint request to Dr. Micah Dembo, Theoretical Division, Los Alamos Scientific Laboratory, University of California, Los Alamos, NM 87545.

0271-6585/81/0102-0205$05.80 

moves, the tail seems to stick from time to time, causing the cell body to stretch, and that retraction fibers are occasionally drawn out from the uropod and can be considerably stretched before detaching from the substrate [Armstrong and Lackie, 1975; Stossel, 1977]. The upper surface of the uropod also appears to be sticky, since small particles such as platelets and bacteria are seen to adhere to these areas [Greenwood, 1969].

Labeling of cell surface proteins on PMNs with the monovalent fluorescent dye Fluorescein isothiocyanate (FITC) demonstrates that during cell motion there is a pronounced redistribution of this marker to the region of the uropod [Ryan et al, 1974]. We will call the brightly fluorescent spots thus formed "monomer caps." Polymerization of surface proteins by agents such as concanavalin A or immunoglobulin will also cause capping (ie, polymer caps).

Ryan et al [1974] report several observations which clearly indicate that monomer caps and polymer caps are formed by different mechanisms. These are: 1) Monomer caps are not endocytized to an observable degree, whereas polymer caps are rapidly endocytized. 2) Monomer caps have an absolute requirement for cell motion, whereas polymer caps do not; inhibition of cell locomotion by agents such as cytoclasin B eliminated monomer caps, although polymer caps were not inhibited. 3) With monomer capping the cells retain a slight diffuse staining over the cell body, whereas polymer caps have a more clearly defined boundary. 4) Monomer caps occur only at the uropod, whereas polymer caps can occur at the uropod or at the center of the cell.

The occurrence of polymer capping and the related phenomenon of centripetal particle transport on moving cells has been attributed to coupling of receptors to a convective flow of the membrane as a whole [Abercrombie et al, 1972; Harris and Dunn, 1972; Bretcher, 1976; Harris, 1976]. It has also been proposed that the membrane as a whole is stationary but that receptors activated by cross-linking can be coupled to the motion of submembrane contractile proteins by means of certain intermediates such as protein x [Bourguignon and Singer, 1977] or calcium binding protein [Klausner et al, 1980].

In our analysis, the occurrence of monomer capping and the stickiness of the uropod are incidental but revealing features of PMN motility. The essential idea is that adhesive sites on a moving cell react with the surface and remain stuck to the surface for some period of time as the cell moves past. This relative motion results in a tendency for adhesive sites to be conveyed toward the tail. When adhesive attachments between the cell and the surface reach the tail, they sometimes result in the stretched-out retraction fibers which extend from the uropod to the surface. As the cell continues to move, however, the tension placed on the adherent sites at the back of the cell eventually becomes sufficient to break off pieces of the tail or to pull the sites free from the surface. Over time, this process can lead to an accumulation of adhesive sites at the rear of the cell, which in effect gives rise to the uropod. This view of the nature of the uropod has been stated previously by Robineaux [1954] and Ramsey [1972b].

All these models of monomer and polymer capping are structurally similar in that they propose that material that reacts with receptors on a cell is subject to transport by convective flow of some other material. We will refer to this general view as the reaction-convection hypothesis.

In the context of cell motion, the external material is the surface over which the cell is moving and the receptors are the adhesive sites that bind to the surface. The coupling between the receptors and the convective flow presumably produces the force responsible for cell motion and the necessity to break receptor-surface bonds at the uropod is responsible for the principal frictional force on a cell.

The question of the frictional force on a cell moving along a surface is important to studies of cell adhesion. In such studies, it is often the hydrodynamic shear force required to remove adherent cells from a surface that is measured as a primary datum [Bell, 1979]. If the bonds holding the cell to the surface cannot break and reform rapidly or if they are rigidly connected to the cytoskeleton, then the cells will remain stationary under hydrodynamic shear until some element of the structure fails. However, if the bonds are not part of a rigid structure, then the cells will slide or roll along the surface, forming and breaking attachments exactly as if they were undergoing normal locomotion. The terminal velocity of such cells will be such that the frictional force just balances the shear force.

In the case of PMNs, these considerations are relevant during the formation of thrombi under flow conditions. Madras et al [1971] have observed that, after attachment at the site of growing thrombi, "white cells were seen to drag over the surface and be appreciably slowed by their attraction to the surface." In addition, Atherton and Born [1972] have made in vivo measurements of the velocity of adherent granulocytes in exposed venules of mice and hamsters. These cells were observed to roll and slide along the walls of the venules with a velocity (10–20 $\mu$/sec) between 10 and 100 times slower than the mean fluid velocity but 100 times faster than granulocytes can move in stationary fluid. This indicates that the fluid is pushing the cells along but that there is considerable friction between the cells and the surface of the blood vessel. The amount of this friction is presumably important in determining the rate of emigration from venules, since the cells must come to a stop before they can move through the vessel wall.

In this paper we shall present quantitative formulations of the various forms of the reaction-convection hypothesis. Our aim is to clarify the predictions of these models concerning the details of receptor redistribution and concerning the frictional force on a moving cell. We will calculate the spatial distribution of adhesive sites on a cell for several important cases. We will look at how this distribution depends on time and on the size, shape, and speed of the cells as well as on other parameters such as the adhesiveness of the surface.

At appropriate points we shall call attention to experiments that test the validity of various models. We will also point out how certain measurements can be interpreted to yield information on quantities such as the rate constants of receptor binding to the surface and the diffusion constants of the receptors in the cell membrane.

We hope that the mathematical formulation and techniques of analysis we utilize for the present simple problem will be instructive to those interested in the treatment of other theories concerning convective flow, diffusion, and chemical reaction of molecules in the cell membrane. The bulk of the mathematical details have been confined to appendices.

## THE MODEL

Let us assume that a rectangular cell of length L and half-width W is moving at uniform velocity v in the positive X direction. We adopt a frame of reference, moving at the same velocity as the cell. Furthermore, we choose the origin of coordinates at the middle of the tail end of the cell (see Fig. 1).

Real cells clearly do not maintain a fixed shape during motion and they frequently do not look rectangular. Nevertheless, the assumption of rectangular geometry captures the essence of the cellular geometry (ie, that the cell has a front, a back, and two sides)

in a way which greatly simplifies the mathematics. The qualitative aspects of the results we shall present do not depend on the details of cell shape.

### Diffusion

In actuality, the cell is three-dimensional, there being an upper membrane in contact with the medium and a lower membrane in contact with the surface. Receptors which are free to diffuse can be on either membrane. Let the number of free receptors per unit area on the upper and lower membranes of the cell be given by $R_u(X, Y)$ and $R_\ell(X, Y)$, respectively. If there are several classes of receptors on the cell we will assume that each class behaves independently of the others.

### Binding and Release of Receptors

We shall assume that the surface contains a large number of sites per unit area, $B_s$, to which receptors on the bottom of the cell can adhere according to the scheme

$$R_\ell + B_s \underset{k_-}{\overset{k_+}{\rightleftharpoons}} C. \tag{1}$$

In Equation (1), $C(X, Y)$ denotes the surface density of receptor-surface bonds and k+ and k– are the forward and reverse rate constants of the binding reaction. Note that both the surface binding sites $B_s$ and the complexes C are fixed with respect to the surface and consequently do not diffuse. This implies that

$$B_s + C = B_o \tag{2}$$

where $B_o$, the total density of sites on the surface, is a constant.

In order to obtain the advantage of a linear model we will neglect those cases where the adhesive sites on a cell saturate a significant fraction of the sites on the surface. This simplification implies that

$$C \ll B_s \cong B_o, \tag{3}$$

so that $B_s$ is approximately constant.

### Membrane Flow

The simplest situation to formulate from a mathematical point of view is the case where receptors are coupled to convective flow of submembrane elements only when they are activated by binding to the surface. Since there is no bulk flow of the membrane under these circumstances, receptors on the upper surface and unbound receptors on the lower surface move only by diffusion. We refer to this model as that of the "sliding cell" (see Fig. 2).

If the cell has a tendency to roll as it moves across the surface, then in the reference frame of the moving cell it will appear that there is a bulk flow of the upper membrane toward the front of the cell and a corresponding flow of the lower membrane toward the rear (similar to a "tank tread"). Note that, if the velocity of the flow of the upper membrane is $v_m$, then continuity of the flow requires that the flow of the lower membrane be $-v_m$.

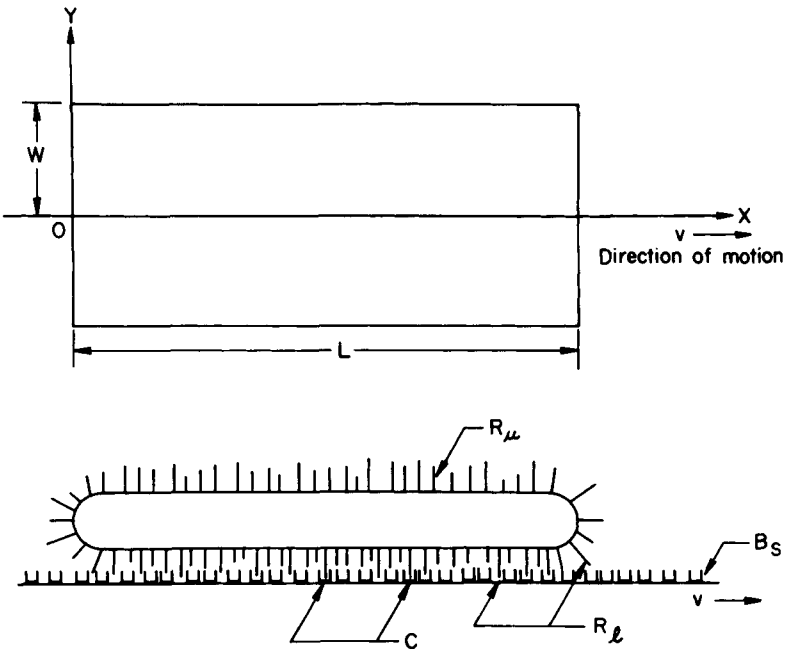


Fig. 1. Top and side view of a cell in contact with a surface. Notation for the dimensions of the cell and for the various states of receptors on the cell are indicated.

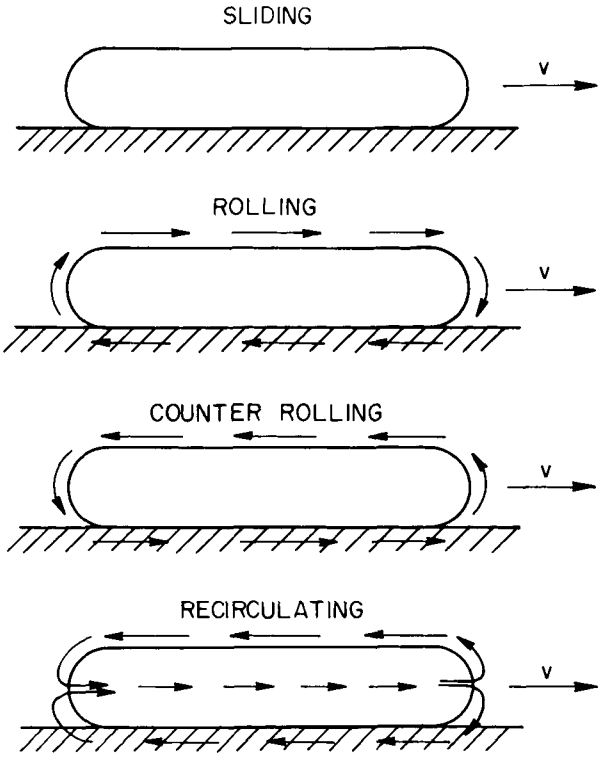


Fig. 2. Several modes of motion of the cell membrane.

Let us define $\delta$ as the ratio of the velocity of membrane flow on the upper surface to the velocity of the cell as a whole,

$$\delta = v_m/v. \tag{4}$$

As shown in Figure 2, if $\delta > 0$ we have the case of the forward rolling cell, if $\delta = 0$ the cell slides with no rolling, and if $\delta < 0$ the cell rolls in a direction counter to its overall motion. It is difficult to think of a physically plausible justification for the case of the counter-rolling cell.

Abercrombie et al [1972] proposed that there was a bulk flow of membrane from the front to the back of moving cells over both the upper and lower membranes. Further support and elaboration of this hypothesis were provided by Harris and Dunn [1972] and Harris [1973]. In this model, it is asserted that the flow of membrane implies the insertion of membrane material at the leading edge of the cell and the resorption of membrane at the tail followed by recycling of the resorbed material back to the leading edge. We will refer to this particular scheme of membrane flow during cell motion as recirculating flow (see Fig. 2).

There is no fundamental difficulty in dealing with the consequences of recirculating flow within the context of the present formalism. Nevertheless, since there is a discontinuity of membrane flow at the front and back boundaries of the cell, recirculating flow is somewhat complicated to formulate mathematically. Therefore, we will initially work out the detailed characteristics of the rolling and sliding cell and after this has been digested we will return, in the last part of the Results section, to the analysis of recirculating flow.

### Differential Equations

We calculate the rates of change of $R_u$, $R_\ell$, and C as seen by an observer moving along with the cell. At every point (X, Y) within the rectangle representing a cell of length L and width 2W, we have contributions from diffusion for $R_u$ and $R_\ell$; contributions from convection to all three quantities; and contributions from association and dissociation with surface sites to $R_\ell$ and C. Writing the terms in that order we have:

$$\frac{\partial R_u}{\partial t} = D\left(\frac{\partial^2}{\partial X^2} + \frac{\partial^2}{\partial Y^2}\right) R_u - \delta v\left(\frac{\partial R_u}{\partial X}\right) \tag{5a}$$

$$\frac{\partial R_\ell}{\partial t} = D\left(\frac{\partial^2}{\partial X^2} + \frac{\partial^2}{\partial Y^2}\right) R_\ell + \delta v\left(\frac{\partial R_\ell}{\partial X}\right) - k_+ B_s R_\ell + k_- C \tag{5b}$$

and

$$\partial C/\partial t = v(\partial C/\partial X) + k_+ B_s R_\ell - k_- C. \tag{5c}$$

### Boundary Conditions

For boundary conditions, we must require continuity of diffusing species along the boundary of the cell

$$R_u(X, Y) = R_\ell(X, Y) \text{ if } Y = \pm W \text{ or if } X = 0 \text{ or } L \tag{6a}$$

If $v \neq 0$, we must also require that the number of receptor-surface complexes at the leading edge of the cell is zero.

$$C(L,Y) = 0 \text{ --- } W \leqslant Y \leqslant W. \tag{6b}$$

In addition, since receptors cannot leave the cell surface, we require that the normal component of the total flux of receptors vanish at the boundaries. Thus, for a rolling or sliding cell,

$$[D\partial(R_u + R_\ell)/\partial X] + vC + \delta v(R_\ell - R_u) = 0 \text{ if } X = 0 \text{ or if } X = L \tag{6c}$$

and

$$D\partial(R_u + R_\ell)/\partial Y = 0 \text{ if } Y = \pm W. \tag{6d}$$

Finally, we note that the geometry of the problem is symmetric to the left and right of the axis along which the cell is moving. Consequently, if the initial conditions are also symmetric, then

$$\partial R_u/\partial Y = \partial R_\ell/\partial Y = \partial C/\partial Y = 0 \text{ at } Y = 0. \tag{6e}$$

### Global Conservation of Receptors

Adding together differential equations a, b, and c, integrating the sum from 0 to L with respect to X and from $-W$ to W with respect to Y and applying boundary conditions (6c) and (6d) shows that the total number of receptors per cell is a constant

$$N = 4WLR_0. \tag{7}$$

In this equation, N is the total number of receptors on the cell and $R_0$ is the average density of receptors on the cell surface.

### Nondimensional Formulation*

$R_0$ provides a convenient scale with which to measure $R_u$, $R_\ell$, and C. Consequently, we introduce nondimensional variables

$$\hat{r}_\ell \equiv R_\ell/R_0, \; \hat{r}_u \equiv R_u/R_0 \text{ and } \hat{c} \equiv C/R_0. \tag{8a}$$

We shall also define nondimensional time

$$\tau = k_+ B_s t \tag{8b}$$

and nondimensional distances

$$x \equiv X/L \text{ and } y \equiv Y/W. \tag{8c}$$

*This section and the following one deal primarily with mathematical issues. They can be skipped without a major loss of continuity.

In terms of these variables, the differential equations (5a–5c) become:

$$\frac{\partial \hat{r}_u}{\partial \tau} = \beta\epsilon\left(\frac{\partial^2}{\partial x^2} + \frac{L^2}{W^2}\frac{\partial^2}{\partial y^2}\right)\hat{r}_u - \delta\beta(\partial \hat{r}_\ell/\partial X) - \hat{r}_\ell + \gamma\hat{c}_\ell \tag{9a}$$

$$\frac{\partial \hat{r}_\ell}{\partial \tau} = \beta\epsilon\left(\frac{\partial^2}{\partial x^2} + \frac{L^2}{W^2}\frac{\partial^2}{\partial y^2}\right)\hat{r}_\ell + \delta\beta(\partial \hat{r}_\ell/\partial x) - \hat{r}_\ell + \gamma\hat{c}_\ell \tag{9b}$$

$$\partial \hat{c}/\partial \tau = \beta(\partial \hat{c}/\partial x) + \hat{r}_\ell - \gamma\hat{c} \tag{9c}$$

where

$$\gamma \equiv k_-/k_+B_s, \quad \beta = v/Lk_+B_s, \quad \text{and} \quad \epsilon = D/vL. \tag{10}$$

For convenience of reference, the fundamental nondimensional parameters of the model are listed and defined in Table II.

### Reduction of Equations to One Space Dimension

If we integrate equations 9a, 9b, and 9c from zero to one with respect to y and apply boundary conditions (6d) and (6e) we obtain

$$\partial r_u/\partial \tau = \beta\epsilon(\partial^2/\partial x^2)r_u + \beta\epsilon\phi(x) - \delta\beta(\partial/\partial x)r_u \tag{11a}$$

$$\partial r_\ell/\partial \tau = \beta\epsilon(\partial^2/\partial x^2)r_\ell - \beta\epsilon\phi(x) + \delta\beta(\partial/\partial x)r_\ell - r_\ell + \gamma c \tag{11b}$$

$$\partial c/\partial \tau = \beta(\partial/\partial x)c + r_\ell - \gamma c \tag{11c}$$

where

$$r_u \equiv \int_0^1 \hat{r}_u\, dy, \quad r_\ell \equiv \int_0^1 \hat{r}_\ell\, dy, \text{ and } c \equiv \int_0^1 \hat{c}\, dy \tag{12}$$

are the average values of $\hat{r}_u$, $\hat{r}_\ell$, and $\hat{c}$ over a cross section of the cell parallel to the y axis and

$$\phi(x,\tau) = (L^2/W^2)(\partial/\partial y)\hat{r}_u(x,1) = -(L^2/W^2)(\partial/\partial y)\hat{r}_\ell(x,1). \tag{13}$$

In Appendix A, we show that an approximate expression for $\phi$ is

$$\phi(x,\tau) \cong \omega^2 L^2/W^2(r_\ell - r_u) \equiv \rho^2(r_\ell - r_u) \tag{14}$$

where $\omega^2 \cong 1.86 \pm 0.62$ and $\rho \equiv \omega L/W$.

Physically, $\phi$ represents the net transport of receptors from the bottom to the top of the cell due to diffusion over the side edges. Equation (14) implies that to first approximation this transport is proportional to the difference between the average number of receptors on the lower and upper surfaces, and that the constant of proportionality is $\rho^2$.

Nondimensionalization of the boundary conditions 6a–6e followed by integration with respect to y between 0 and 1 yields the following boundary conditions on Equations 11a–11c.

$$r_u = r_\ell \text{ at } x = 0, 1 \tag{15a}$$

$$\epsilon(\partial/\partial x)(r_u + r_\ell) + c = 0 \text{ at } x = 0, 1 \tag{15b}$$

and

$$c = 0 \text{ at } x = 1. \tag{15c}$$

### The Frictional Force

From the discussion in the Introduction it is clear that the frictional force on a cell will be somehow related to the number of adhesive bonds to the surface that must be broken per unit time as the cell moves. This idea can be formulated in a precise way if we assume that when a membrane-surface bond reaches the tail of the cell it results in the formation of a microscopic retraction fiber which exists for a short time before the membrane-surface bond ruptures.* If each fiber is identical and tends to retard the forward motion of the cell by an equal amount, then the total frictional force on the cell will be proportional to the number of such fibers.

$$F_r = \Omega N_{fib}. \tag{16}$$

In this equation $N_{fib}$ is the number of retraction fibers per cell and $\Omega$ is the force with which a retraction fiber pulls on the cell. It is also clear that, before it ruptures, the forces on a membrane-surface bond must balance, so that $\Omega$ is equal to the force tending to cause rupture of this bond.

If a bond is under stress due to an applied force, $\Omega$, then the probability per unit time that it will rupture is increased by this force according to a relation of the form [Bell, 1978, 1979],

$$k_{rup} = k_- \exp [\Omega/\theta], \tag{17}$$

where $k_-$ is the rate constant for spontaneous rupture and $\theta$ is a constant that characterizes the bond with respect to its ability to resist stress.

*Although it is convenient for purposes of exposition to assume the existence of retraction fibers, our considerations are independent of the mechanism by which the force between the bound receptor and the substratum is transmitted to the remainder of the cell.

Since the rate at which bonds reach the back edge of a moving cell is given by $v\int_{-W}^{W} C(0, Y)dY$, the number of fibers pulling on the cell at any given time will satisfy the differential equation

$$(d/dt)N_{fib} = v\int_{-W}^{W} C(0, Y)dY - k_{rup}N_{fib}. \tag{18}$$

Consequently, when $N_{fib}$ is in steady state, $d/dt\ N_{fib} = 0$, and

$$N_{fib} = \frac{v\int_{-W}^{W} C(0, Y)dY}{k_{rup}}. \tag{19}$$

Adding together the forces produced by each retraction fiber, we see that the total frictional force on a cell in steady motion is

$$F_r = \Omega N_{fib} = \frac{v\int_{-W}^{W} C(0, Y)dY}{k_-}\left\{\Omega \exp\left[-\Omega/\theta\right]\right\}. \tag{20}$$

Note that $F_r$ is proportional to the cell velocity as in first approximation a frictional force must be.

Since $\Omega$ and $\theta$ are constants, the term in brackets in Equation (20) is a constant with units of force which we will call $\Omega'$. We also find it convenient to define the nondimensional frictional force per cell surface receptor as

$$f_r \equiv F_r/[N\Omega'].* \tag{21}$$

In terms of the nondimensional variables defined in Equation (10), Equation (21) becomes

$$f_r = \beta c(0)/2\gamma \tag{22}$$

## METHODS

In the figures which follow the solid dots represent the results of numerical integration of Equations 11–15. Finite differences were used to approximate derivatives with respect to the space variable, x. Increasingly finer grid points were used near the boundaries owing to the occurrence of boundary layers. This procedure reduced the partial differential equations to a large system of ordinary differential equations which were then solved using the method of Gear [1973].

## RESULTS

### The Sliding Cell

We will initially concentrate our analysis on the special case of cells moving in the absence of membrane flow. Thus, it will be assumed that there is no rolling of the cells and that no recirculation of membrane takes place. We will present some results concerning rolling and recirculation after we have finished with the sliding cell.

*Recall that $N = 4LWR_0$ is the total number of receptors per cell.

Table I presents typical values of the relevant parameters of the sliding cell model for the case of human PMNs. As can be seen from this table, most of the parameters (ie, L, W, v, $v_m$, and D) can be fixed to within at least an order of magnitude on the basis of previous work. The only parameters that are unknown in advance are the rate constants for dissociation and binding of receptors and the surface, $k_-$ and $k_+B_s$. Very little is known about these quantities since the chemical natures and density of the receptors on the cell and of the surface binding sites are unknown. Nonetheless, as initial guesses for $k_-$ and $k_+B_s$, Table I gives the estimates of Bell [1978] and Bell [1979]. These estimates are based on the presumption that receptor-surface bonds are similar to antibody-hapten or lectin-monosaccaride bonds and that the density of sites on the surface is similar to other surface densities commonly encountered in biology (eg, the density of cell surface antibody molecules on B cells or the density of Con A receptors).

Table II lists the nondimensional parameters of the model together with the values corresponding to the estimated dimensioned parameters of Table I. As can be seen from this table, $k_-$ and $k_+B_s$ occur only in the definitions of $\beta$ and $\gamma$. We shall examine the predictions of the model for all possible values of $\beta$ and $\gamma$ and compare these predictions with experiment in order to narrow the range of acceptable values for the unknown elements of the model.

**TABLE I. Parameters of the Model for the Case of the Sliding Cell***

| Parameter | Symbol | Best estimate | Range | Reference |
|---|---|---|---|---|
| Length of cell | L | $3 \times 10^{-3}$ cm | $1.5–5 \times 10^{-3}$ | (1, 2, 3) |
| Width of cell[a] | 2W | $7.5 \times 10^{-4}$ cm | $5–10 \times 10^{-4}$ cm | (1, 2, 3) |
| Velocity of cell motion | v | $2 \times 10^{-5}$ cm/sec | $1–5 \times 10^{-5}$ cm/sec | (3, 4) |
| Velocity of membrane motion due to rolling[b] | $v_m$ | 0 | 0 | (5) |
| Diffusion constant of cell surface receptors | D | $10^{-10}$ cm²/sec | $10^{-9}–10^{-11}$ cm²/sec | (6, 7) |
| Rate constant of receptor-surface binding | $k_+B_s$ | 1 $sec^{-1}$ | $10^{-5}–10^{5}$ $sec^{-1}$ | (8, 9) |
| Rate constant of receptor-surface dissociation | $k_-$ | 1 $sec^{-1}$ | $10^{-5}–10^{5}$ $sec^{-1}$ | (8, 9) |

*Applicable to human PMNs during spontaneous random or chemotactic motion under conditions of in vitro observation.

[a]Recall that W is defined as one-half the width of the cell.

[b]Rolling of cells has been observed only under in vivo conditions involving fluid flow; consequently we assume in the first part of the Results section that $v_m = 0$ so that the cell slides without rolling. Subsequently, we consider the cases of $v_m \neq 0$ both for cell rolling and for membrane recirculation.

References: 1) Ryan et al [1978], 2) Ramsey [1972b], 3) Senda et al [1975], 4) Ramsey [1972a], 5) Atherton and Born [1972], 6) Elson et al [1976], 7) Cherry [1979], 8) Bell [1979], 9) Bell [1978].

**TABLE II. Nondimensional Parameters of the Model**

| |
|---|
| $\rho^a \equiv \omega L/W \cong 10$ |
| $\epsilon \equiv D/vL \cong 2 \times 10^{-3}$ |
| $\beta \equiv v/Lk_+B_s \cong 10^{-2}$ |
| $\gamma \equiv k_-/k_+B_s \cong 1$ |
| $\delta^b = v_m/v \cong 0$ |

[a]As shown in Appendix A, $\omega^2 \cong 1.86$.

[b]This is for the case of the sliding cell. $\delta \approx 1$ for the rolling cell and $\delta \sim -0.25$ for the recirculating membrane.

Figure 3 illustrates the way in which the distribution of the total receptor density, $r_{tot}(x) = r_u + r_\ell + c$, changes with time. In this computation, the nondimensional parameters were chosen as shown in Table II, and the cell was assumed to be initially stationary and at equilibrium with the surface.

It can be seen from Figure 3 that there is a progressive transport of receptors toward the rear of the cell after it begins to move. This transport eventually leads to the development of a stable gradient from the tail to the front of the cell in which there is a $\gtrsim$10-fold increase in the density of receptors at the tail of the moving cell as opposed to the resting cell. It is clear that an effect of this magnitude is sufficient to account for the observation of monomer capping of cell surface proteins labeled with monovalent fluorescent dyes [Ryan et al, 1974].

In order to gauge the "real" time necessary for the redistribution shown in Figure 3 to occur, we note that the nondimensional time required is $\tau \approx 100$. The number of cell lengths moved in this time is $\beta\tau \cong 1$. Thus, the model shows that for appropriate parameter values monomer capping can be completed in the time it takes for the cell to move 1–10 cell lengths. Reference to the values of v and L in Table I shows that this time is on the order of a few minutes. This is certainly a desirable feature since Ryan et al [1974] have

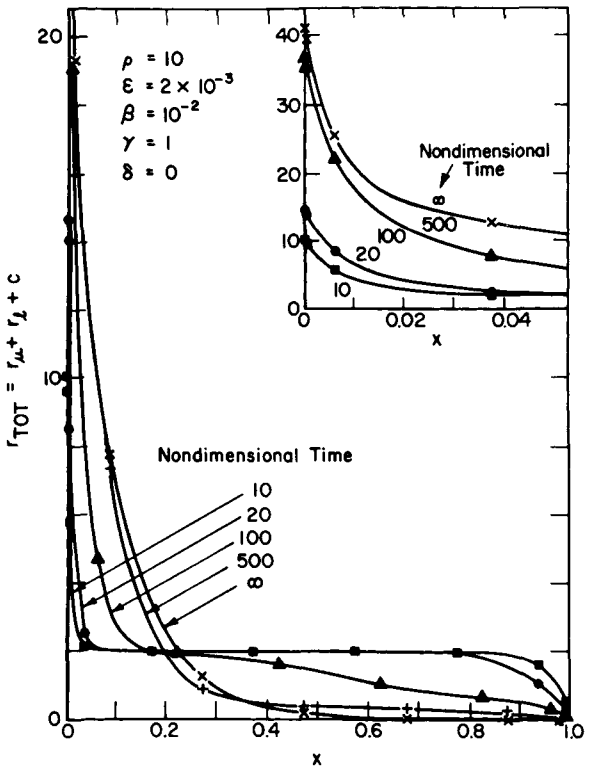


Fig. 3. Numerical computation of the time course of receptor redistribution for the parameter values in Table II.

observed that monomer caps are formed and fairly stable in 5 minutes. Since a stable distribution is reached so rapidly, we will henceforth restrict our discussion to the equilibrium properties of the model.

Figure 4 shows how the equilibrium (ie, $t = \infty$) distribution of $r_{tot}$ depends on the velocity of cell motion assuming other parameters are fixed. This is equivalent to varying $\beta$ in direct proportion to v while holding $\rho$, $\gamma$ and the product $\epsilon\beta$ fixed.

Figure 4 shows that, as v gets large, there is a progressive increase in the density of receptors at the back versus the front of the cell. Furthermore, the redistribution is saturable so that, after a certain point, further increases in the velocity of the cell produce a negligible change in the overall pattern of redistribution.

Figure 4 also shows that as $v \to 0$, the receptors are uniformly distributed over the cell and that $r_{tot} = 2$. The reason for this is clear from the solution to Equation (11) for the trivial special case $\beta = 0$,

$$r_\ell = r_u = 2\gamma/(1 + 2\gamma) \tag{23}$$

and

$$c = 2/(1 + 2\gamma). \tag{24}$$

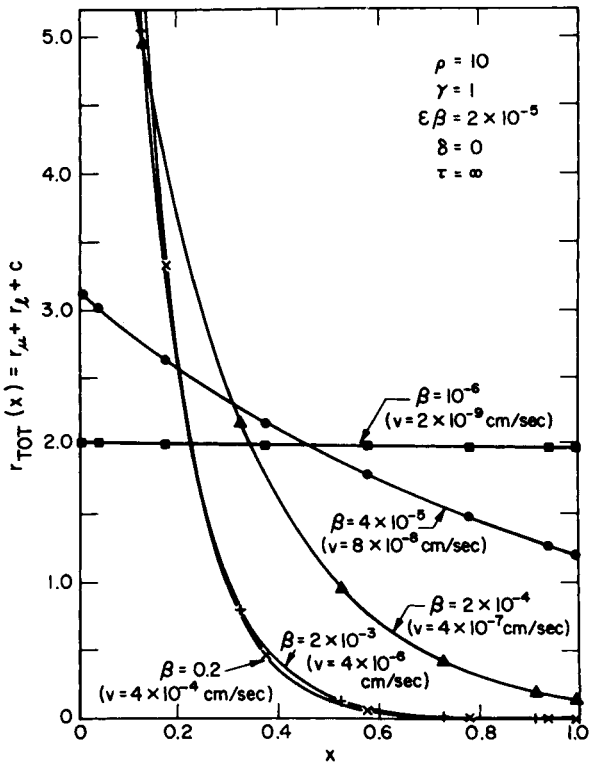


Fig. 4. Effect of the velocity of cell motion on the equilibrium distribution of receptors. Parameters other than v were fixed at values given in Table I.

Thus, when the cell is stationary, $r_\ell$, $r_u$, and c are uniform and depend only on the dissociation constant, $\gamma$. As a consequence of this behavior, measurement of the densities of receptors on the upper or lower surface of a stationary cell should provide the most direct way to determine $\gamma$.

If $B_s$ can be varied, for example, by coating the surface with various mixtures of albumin and fibronectin, then by measuring $\gamma$ on a series of such surfaces, the dimensional binding constant $k_+/k_-$ can also be determined.

Superficially, the result that receptor redistribution for the sliding cell model requires cell motion seems to contradict the experimental observation that capping of Con A can occur on stationary cells. This is not a real contradiction because, in the case of cell motion, the external ligand (ie, the surface) has infinite mass, whereas the mass of a Con A molecule is negligible. The infinite mass of the surface means that a bound receptor must be stationary with respect to the observer even though it may experience a considerable force. Therefore, if the cell is also stationary, there can be no redistribution of receptors. The small mass of Con A means that a bound receptor is not held stationary with respect to the observer. Thus, if Con A (or some other small object) induces receptor coupling to submembrane contractile proteins on a stationary cell, receptor redistribution is a natural consequence.

Since $r_{tot} = 2$ everywhere on a nonmoving cell independent of the choice of parameters, the relative change in the density of receptors at the tail of a moving versus nonmoving cell provides a useful measure of the degree of receptor redistribution in terms of a single quantity. Figure 5 shows the way in which $r_{tot}(0)$ depends on the unknown parameters $\beta$ and $\gamma$ when $\rho$ and $\epsilon$ are fixed at the values given in Table II. As can be seen from this figure, the amount of redistribution approaches a maximum as $\gamma$ and $\beta$ go to zero. Also, if $\gamma > 10^2$ or if $\beta > 10^2$, then the amount of receptor redistribution is insignificant. For a given curve in Figure 5, increasing $\beta = v/L k_+ B_s$ corresponds to decreasing $k_+ B_s$ and $k_-$ in proportion, thus slowing the binding kinetics while preserving the equilibrium rate constant ratio $\gamma = k_-/k_+ B_s$. This is in contrast to Figure 4, where increasing $\beta$ should be interpreted as representing increasing cell speed.

The reason for the properties of receptor redistribution illustrated in Figures 3–5 can be understood qualitatively by means of a simple physical argument. The lifetime of a receptor-surface complex is $1/k_-$, and since the complex moves to the tail with velocity v, the distance it moves during its lifetime is $\cong v/k_-$. Since the cell is of length L, the number of times a typical receptor binds to the surface before reaching the tail is $\cong 1 + Lk_-/v = 1 + \gamma/\beta$. This quantity is important, since between the times that a receptor is attached to the surface and moving toward the rear, it diffuses with zero average displacement, essentially waiting for its next opportunity to bind. The number of such waiting periods is $(\beta + \gamma)/\beta$ and their average duration is $(k_+ B_s)^{-1}$, so that the time spent waiting is $\cong(\beta + \gamma)/(k_+ B_s \beta)$. The time required to move to the tail, neglecting the waiting period, is simply $L/v = (k_+ B_s \beta)^{-1}$. Thus, the total time required to move to the tail for a typical receptor is $\tau_1 \cong (1 + \gamma + \beta)/(\beta k_+ B_s)$. Opposing the tendency for redistribution toward the tail is the tendency of the receptors to spread over the cell by diffusion. This occurs with characteristic time $\tau_2 \cong L^2/D = [\beta \epsilon k_+ B_s]^{-1}$. Clearly, in order for redistribution to dominate, $\tau_1$ must be much less than $\tau_2$, or in nondimensional terms

$$\epsilon[1 + \beta + \gamma] \ll 1. \tag{25}$$

This equation represents the basic criterion for the occurrence of receptor redistribution on a sliding cell. It demonstrates that, for fixed $\epsilon$, redistribution will approach a max-

imum as $\beta$ and/or $\gamma$ go to zero and will decrease as $\beta$ and/or $\gamma$ get large. This accounts for the gradual decline of the curves in Figure 5 as well as for the absence of significant redistribution when $\gamma \cong 10^2$.

Under the condition of inequality (Equation 25) an approximate analytic solution to Equation (11) at steady state can be derived by means of boundary layer theory (see Appendix B). The resulting expressions for $r_u$, $r_\ell$, and c correct to $0[(\epsilon\gamma)^2]$ are:

$$(1/A)r_u = [\cosh(\rho x) - \coth(\rho)\sinh(\rho x)](1 + \tfrac{1}{2}\gamma\epsilon\rho^2 x) + \gamma\epsilon\rho\left[\frac{\lambda_+ + 1}{\lambda_+}\right]\frac{\sinh(x)}{\sinh^2(\rho)} \tag{26a}$$

$$(1/A)r_\ell = [1 - \gamma\epsilon\rho\coth(\rho)]\exp(x\lambda_-/\gamma\epsilon) + \gamma\epsilon\rho\,[\coth(\rho)\cosh(\rho x) - \sinh(\rho x)] + [\delta\epsilon\rho/\lambda_+\sinh(\rho)]\exp[(x-1)\lambda_+/\gamma\epsilon] \tag{26b}$$

and

$$(1/A)c = (-\epsilon/A)\partial_x(r_u + r_\ell) = [-(1/\gamma) + \epsilon\rho\coth(\rho)]\lambda_- \exp[(\lambda_- x/\gamma\epsilon)] - [\epsilon\rho/\sinh(\rho)]\exp[(x-1)\lambda_+/\gamma\epsilon] + \epsilon\rho[\coth(\rho)\cosh(\rho x) - \sinh(\rho x)] \tag{26c}$$

where

$$\lambda_\pm = \tfrac{1}{2}(\epsilon\gamma^2/\beta)(1 \pm \sqrt{1 + 4(\beta/\epsilon\gamma^2)}\,). \tag{26d}$$

Note that from Equations (26a) and (26b), "A" has the physical significance of being the common value of $r_\ell$ and $r_u$ at $x = 0$. $A^{-1}$ is given to order $(\epsilon\gamma)^2$ by

$$\frac{1}{A} = \frac{1}{2}\left[\frac{\cosh(\rho) - 1}{\rho\sinh(\rho)} + \epsilon\gamma\left(\frac{(\sinh(\rho) - (\rho)}{2\sinh(\rho)} + \left(\frac{\lambda_+ + 1}{\lambda_+}\right)\frac{(\cosh(\rho) - 1)}{\rho\sinh^2(\rho)} + \frac{(2\lambda_- + \gamma\lambda_- - \gamma)}{\gamma\lambda_-}\right)\right]. \tag{26e}$$

Figures 6–8 show the agreement between the analytic solution and numerical solution for the parameter values in Table II. There are several notable details of the distributions of $r_u$, $r_\ell$, and c over the cell. First, as remarked previously, all three densities fall as one moves from the tail to the front of the cell; however, $r_u$ falls slowly compared to $r_\ell$ and c. Equation (26) shows that this behavior is due to the existence of a boundary layer of thickness $\epsilon\gamma L/\lambda_-$ at the rear of the cell in which $r_\ell$ and c fall rapidly to the limiting values of $\gamma\epsilon\rho\coth\rho$ and $\epsilon\rho\coth\rho$, respectively, whereas in comparison $r_u$ remains approximately constant (see inserts in Figs. 7 and 8). Outside of this boundary layer under the main body of the cell, c(x) and $r_\ell(x)$ are in quasi-chemical equilibrium; ie, $r_\ell(x) \cong \gamma c(x)$. This condition persists until very close to the front of the cell, where there is another boundary layer of thickness $\epsilon\gamma L/\lambda_+$. The behavior in this leading boundary layer is illustrated by the inserts in Figures 6–8; as shown, c(x) falls to zero whereas $r_\ell(x)$ undergoes a slight rise.

In light of Equation (26), information on the parameters of the model can be obtained by appropriate observations on the distribution of receptors on moving cells. For example, interference contrast microscopy of moving PMNs shows that the majority of

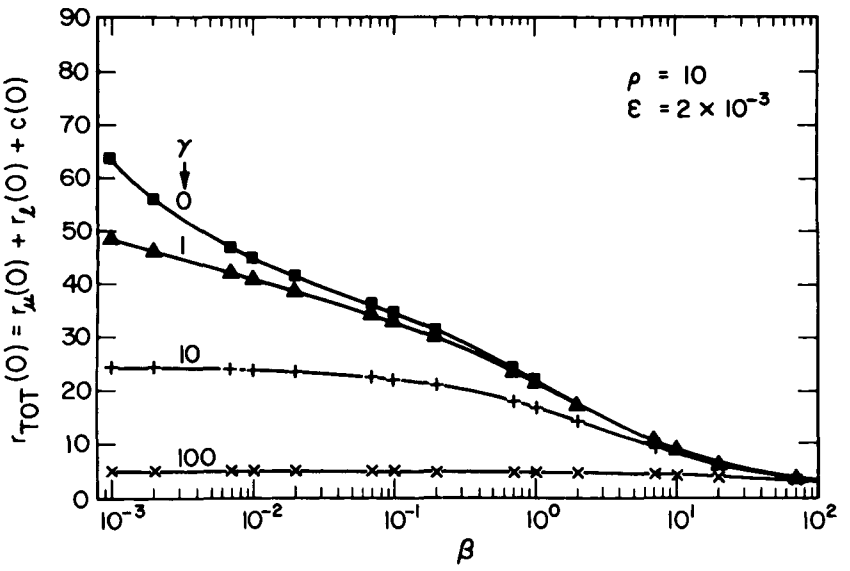


Fig. 5. Numerical computation of the dependence of the total receptor density at x = 0, [$r_{tot}(0) = r_u(0) + r_\ell(0) + c(0)$], on $\beta = v/(k+B_S L)$ as $k+B_S$ and $k_-$ are decreased so that the ratio $\gamma = k/(k+B_S)$ is held constant. The various curves correspond to several choices for the value of $\gamma$ between 0 and 100. The other parameters of the model ($\epsilon$, $\rho$, and $\delta$) are as given in Table II. The figure shows that receptor redistribution requires that both $\gamma$ and $\beta$ be of order 10 or less.

the lower surface of the cell is in moderately close contact with the surface although there are no zones of very tight adherence such as those found on fibroblasts. At the leading margin of the cell there is an area of weak or loose contact with the surface which is seen to fluctuate rapidly, indicating the absence of a significant density of bonds holding these areas to the surface [Armstrong and Lackie, 1975; King et al, 1980]. If we equate the average size of the areas of weak attachments with the size of the leading boundary layer, then the value of $L\epsilon\gamma/\lambda_+$ can be determined.

According to the model, the density of bonds holding the cell to the surface will rise by an order of magnitude or more in the trailing boundary layer. Consequently, the tail of a moving cell will be stuck more firmly to the surface than will the anterior region. This is in accord with the observations of Armstrong and Lackie [1975] and King et al [1980]. The size of the region of close attachment provides a measure of the size of the boundary layer at the tail of the cell (ie, $\gamma\epsilon L/\lambda_-$).

The predictions of the sliding cell model concerning the frictional force on a cell are most directly revealed in experiments in which cells are exposed to a constant shear force, $F_S$, and their terminal sliding velocity, v, is measured. Thus, we shall be mainly concerned with inverting Equation (22) in order to solve for the velocity in terms of the force. The main difficulty in this procedure arises because the frictional force is proportional to the value of c(0), and c(0) is affected by the velocity in a highly nonlinear way.

An approximate relationship between the terminal velocity and the applied force when the applied force is very small can be obtained by substituting the expression for

c(0) on a stationary cell (Equation 24) into Equation (22). Solving the resulting expression for $\beta$ we obtain

$$\beta \cong (1 + 2\gamma)\gamma f_s, \quad f_s \to 0 \tag{27}$$

where $f_s = F_s(\Omega' N)^{-1}$ is the nondimensional shear force.

If v is sufficiently large, then the condition for receptor redistribution (Equation 25) is valid, the c(0) can be approximated by means of Equation (26c). In this case, the relationship between $\beta$ and $f_s$ is

$$\beta \cong 2A\gamma^2(\epsilon\beta)f_s/[A^2(\epsilon\beta) - 4f_s^2\gamma^2] \tag{28}$$

where A is given by Equation (26e), and we recall that the product $\epsilon\beta$ is independent of v. Equation (28) shows that as the shear force approaches the critical value of

$$f_s^c \cong (A/2\gamma)\sqrt{\epsilon\beta} \tag{29}$$

the velocity of the cell gets very large.

Since an infinite cell velocity is not physically possible, the singularity in Equation (28) means that there must be an abrupt change in the way in which the cell interacts with the surface. This change could involve the cell's being torn free of the surface, or the cell could change its mode of moving across the surface by beginning to roll.

### The Rolling Cell

Figure 9 shows a numerical simulation of the dependence of nondimensional cell velocity (ie, $\beta$) on $f_s$ for the rolling and sliding cells. The parameters $\gamma$, $\rho$, and $\epsilon\beta$ are fixed at the values given in Table II. As shown, the two curves are identical at very low shear forces. This is because c(0) is approximately constant in this region so that both curves are in agreement with Equation (27). Also, as intuition suggests, at moderate shear forces the velocity of a rolling cell is higher than the velocity of a sliding cell. This condition persists until the two curves cross at a point very close to the singularity in the curve for $\delta = 0$. The position of this singularity is in good agreement with Equation (29). At shear forces above the critical level, the rolling motion is the only kind of steady motion possible.

The absence of a singularity in the cell velocity if $\delta = 1$ is due to the effect of cell rolling on the distribution of receptors. This is illustrated in Figure 10. As shown, rolling tends to counteract the accumulation of receptors at the tail, and receptors are more or less evenly distributed over the cell. This means that c(0) will have a much weaker dependence on v if $\delta = 1$ than if $\delta = 0$. Consequently, if $\delta = 1$, $\beta$ will be given to a good approximation by Equation (27); ie, it will be a simple linear function of $f_s$ with no singularities.

### Recirculating Membrane Flow

The nondimensional form of the differential equations governing reaction-convection and diffusion of $r_u$, $r_\ell$, and c for recirculating membrane flow are almost identical to the corresponding differential equations for the sliding or rolling cell (Equations 11a–11c). The only change is that the sign of the term $\delta\beta(\partial r_\ell/\partial x)$ in Equation (11b) is minus instead of plus. This is because for recirculating flow, both the upper and lower membranes move in the same direction.

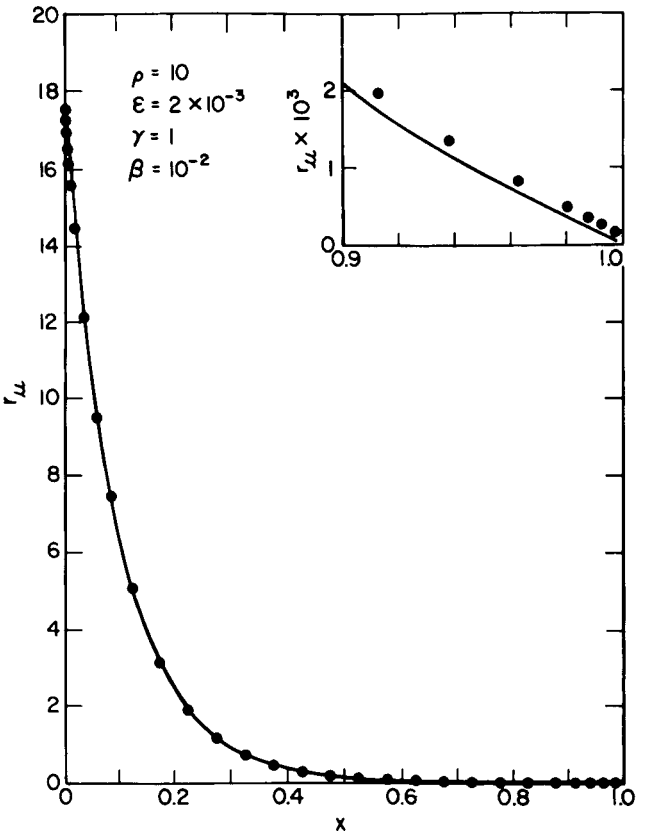


Figs. 6–8. Comparison of numerical and approximate analytic solutions for $r_u$, $r_\ell$, and c. The solid lines were calculated using Equation (26), whereas the closed circles give the corresponding numerical results. Parameter values were fixed at the values given in Table II. The inserts in the figures show the detailed behavior of $r_u$, $r_\ell$, and c in the boundary layers at x = 0 and at x = 1.

It is a more delicate matter to formulate correctly the boundary conditions for recirculating flow due to the discontinuity at the leading and trailing edges. It will still be correct to assume that there is continuity of diffusing species over the boundaries and that the number of bonds at the leading edge is zero (ie, Equations 15a and 15c). However, there is uncertainty as to the remaining boundary conditions.

It seems to us that it is most reasonable to assume that adhesive sites at the tail are resorbed at a rate which is proportional to the local density of these sites. If this is true, then the nondimensionalized condition of zero net flux at the tail (ie, Equation 15b with x = 0) becomes:

$$(\epsilon\partial/\partial x)(r_u + r_\ell) - \delta(r_u + r_\ell) + c = -\lambda\delta(r_u + r_\ell),\ x = 0. \tag{30}$$

Physically, the resorption at the tail can be thought of as similar to flow of a mixture of membrane components through a gel column or filter which retards the passage of receptors somewhat more or less than that of the rest of the membrane. λ measures the ease with which the receptors are resorbed relative to the "average" rate of membrane resorption. If λ = 1, then the receptors are resorbed at the same rate as other components of

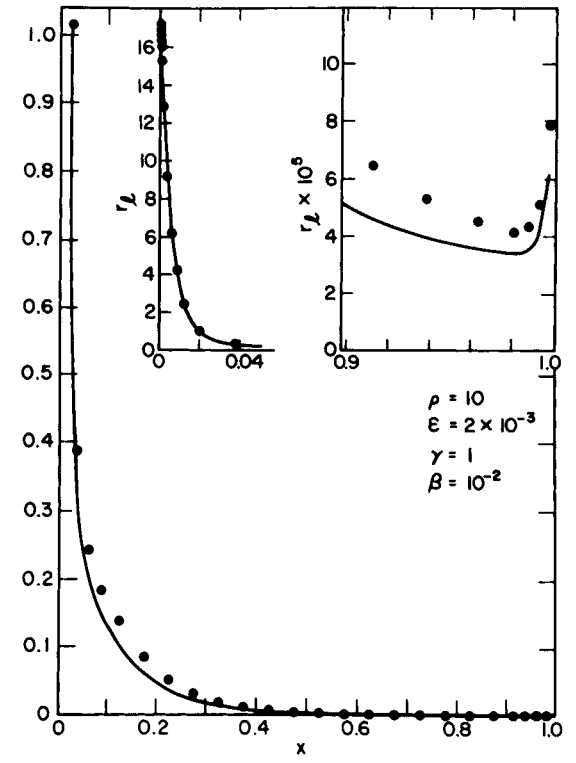
1.0
0.9
0.8
0.7
0.6
0.5
0.4
0.3
0.2
0.1
0
0.2
0.4
0.6
0.8
1.0
x
$r_L$
$r_L \times 10^5$
$\rho = 10$
$\varepsilon = 2 \times 10^{-3}$
$\gamma = 1$
$\beta = 10^{-2}$

Fig. 7.

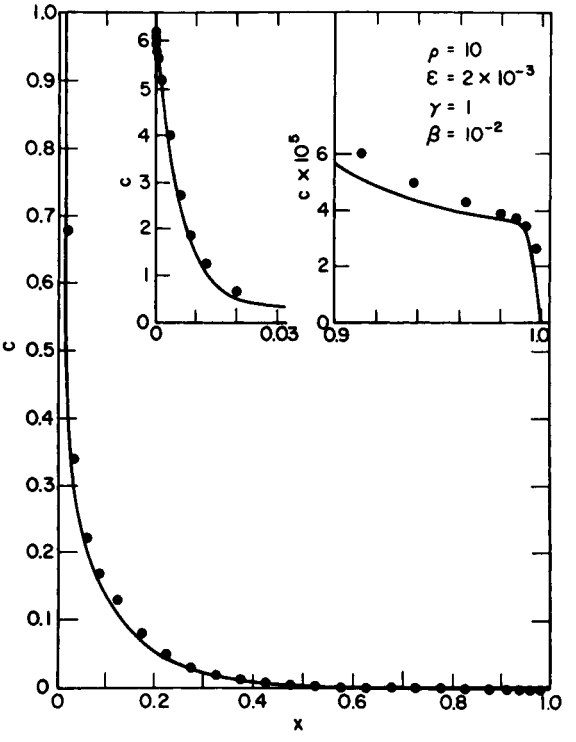
c
x
$c \times 10^5$
$\rho = 10$
$\varepsilon = 2 \times 10^{-3}$
$\gamma = 1$
$\beta = 10^{-2}$

Fig. 8.

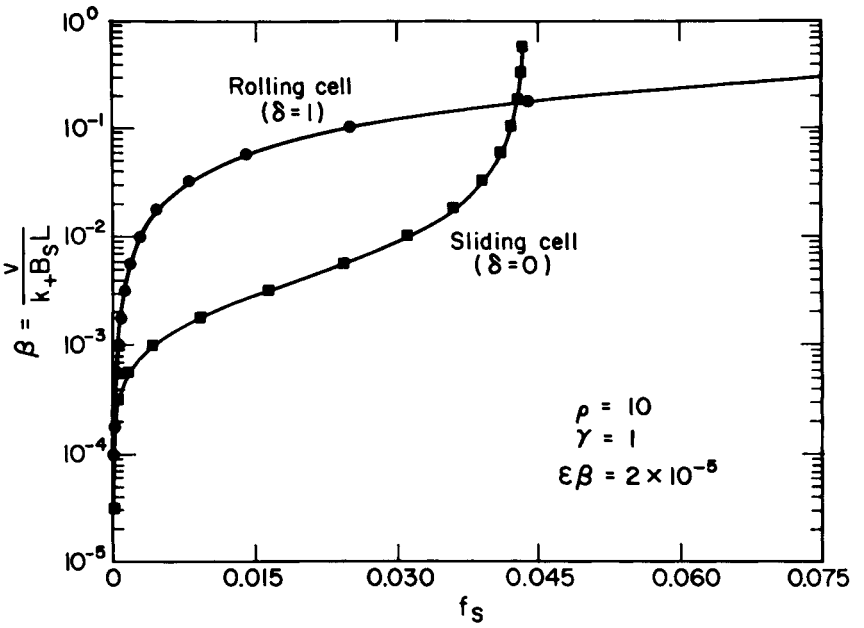


Fig. 9. Comparative dependence of the nondimensional velocity [$\beta = v/(k_+B_SL)$] on the nondimensional shear force [$f_S = F_S/(\Omega' N)$] for the rolling and sliding cells (Equation 10). Changes in receptor distribution as a cell goes from sliding motion ($\delta = 0$) to rolling motion ($\delta = 1$). Parameters other than $\delta$ are as shown in Table II.

the membrane, whereas if $\lambda = 0$ the receptors will be completely excluded from the resorption process. $\lambda > 1$ corresponds to the situation where sites are resorbed more easily than the rest of the membrane. This view of membrane disassembly at the uropod is a generalization that includes the models of Bretcher [1976] and of Harris [1976] as special cases.

If sites are inserted at the leading edge at a rate that is substantially slower than the rate of resorption, then adhesive sites will disappear from the surface and accumulate inside the cell. However, since such disappearance of sites has not been observed, and since monomer caps are stable for long periods of time, we conclude that, if recirculating flow occurs, then the cell must be capable of inserting sites at the leading edge very shortly after they are taken in at the tail, and that very few sites accumulate in the cytoplasm. Thus, the boundary condition for zero flux at the leading edge (Equation 15b with $x = 1$) becomes

$$(\epsilon\partial/\partial x)(r_u + r_\ell) - \delta(r_u + r_\ell) + c = -\lambda\delta[r_u(0) + r_\ell(0)], \; x = 1. \tag{31}$$

One can check that with boundary conditions (Equations 30 and 31) the conservation law of total receptor number holds, and that as a consequence the nondimensional formulation of the differential equations is still consistent.

The parameter values of Tables I and II applicable for the sliding cell are also applicable for recirculating flow with the exception that $v_m \approx -5 \times 10^{-6}$ cm/sec [Harris, 1973] so that $\delta \approx -0.25$. For this range of parameter values, we can obtain approximate analytic solutions for the distribution of receptors for recirculating flow by a derivation very similar

to that given in Appendix B for the case of the sliding cell. The resulting expressions for $r_u$, $r_\ell$, and c good to order $(\epsilon/\delta)$ are*

$$(1/A)r_u \approx \lambda + (1-\lambda)\exp[\delta x/\epsilon] \tag{32a}$$

$$(1/A)r_\ell \approx \lambda(1-\delta\gamma)^{-1}\exp[(1-\delta\gamma)/\beta\delta]\{\exp[-(1-\delta\gamma)x/\beta\delta] - \exp[\delta x/\epsilon]\} + \delta\gamma\lambda(1-\delta\gamma)^{-1}(\exp[\delta x/\epsilon]-1) + \exp[\delta x/\epsilon] \tag{32b}$$

$$(1/A)c \approx \lambda\delta(1-\gamma\delta)^{-1}(\exp[(1-\gamma\delta)(1-x)/\beta\delta]-1), \tag{32c}$$

where A is a constant of proportionality given by

$$1/A = \tfrac{1}{2}\lambda[\beta\delta(1-\gamma\delta)^{-2}(1+\delta)(\exp[(1-\gamma\delta)/\beta\delta]-1) + (1-\gamma\delta)^{-1}(1-2\gamma\delta-\delta)] - \tfrac{1}{2}[\epsilon(\delta(1-\gamma\delta))^{-1}[2(1-\gamma\delta(1-\lambda)) + \lambda(\exp[(1-\gamma\delta)/\beta\delta]-1)]. \tag{32d}$$

Examination of Equations (32a–32d) reveals several distinctive features of receptor redistribution for recirculation flow. These are 1) redistribution will not occur unless $\lambda \ll 1$. Thus, redistribution is essentially caused by the "bottleneck" in the flow of receptors produced if resorption at the tail is difficult. This provides a natural explanation for the role of polymerization or fluorescent labeling of receptors in capping. It is easy to see why modified surface markers of any kind would have a harder time passing through the bottleneck associated with resorption. 2) The density of bonds holding the cell to the surface, c, does not go through a sharp rise at the trailing edge of the cell. This is in contrast to the behavior of c on the sliding cell (Equation 32c). We feel that the absence of such a boundary layer at the tail is an undesirable consequence of recirculating flow hypothesis. Recent observations clearly indicate that the tail is much more firmly stuck to the surface than the mid-portion of the cell [King et al, 1980]. 3) The density of free sites on the upper surface of the cell, $r_u$, undergoes a sharp drop at the tail of the cell if recirculating flow occurs. This boundary layer, of thickness $\sim L\epsilon/\delta$, is not predicted for the case of the sliding or rolling cells. In the case of the sliding cell (Equation 26), $r_u$ fell more slowly with decay constant $\sim\rho$ owing to the effect of diffusion over the side edges. In the case of recirculating flow, the effect of diffusion over the side edges of the cell is negligible so the $\rho$ does not appear in Equation (32a–32d).

An additional aspect of recirculating flow is that receptor redistribution is possible even if binding to the surface does not occur ($\gamma \to \infty$) or if the cell is stationary ($\delta \to -\infty$, $\delta\beta$ and $\epsilon/\delta$ fixed). This provides a good explanation for polymer capping on stationary cells or on cells in suspension. However, the hypothesis does not explain why monomer capping should not also occur on such cells, since it occurs on moving cells [Harris, 1976].

Recently, Middleton [1979] has shown by pulse-labeling with fluorescenated antibody that at least one freely diffusing cell surface marker (ie, the Thy-1 alloantigen) is not swept to the tail during cell motion. This marker was found to redistribute only if it was cross-linked by a second layer of antibody specific for the fluoresceinated antibody.

*This expansion necessarily excludes the possibility of taking the limit $v_m \to 0$. Thus, although recirculating membrane clearly approaches the sliding membrane as $v_m \to 0$, we should not expect Equations (32) to approach Equations (26).

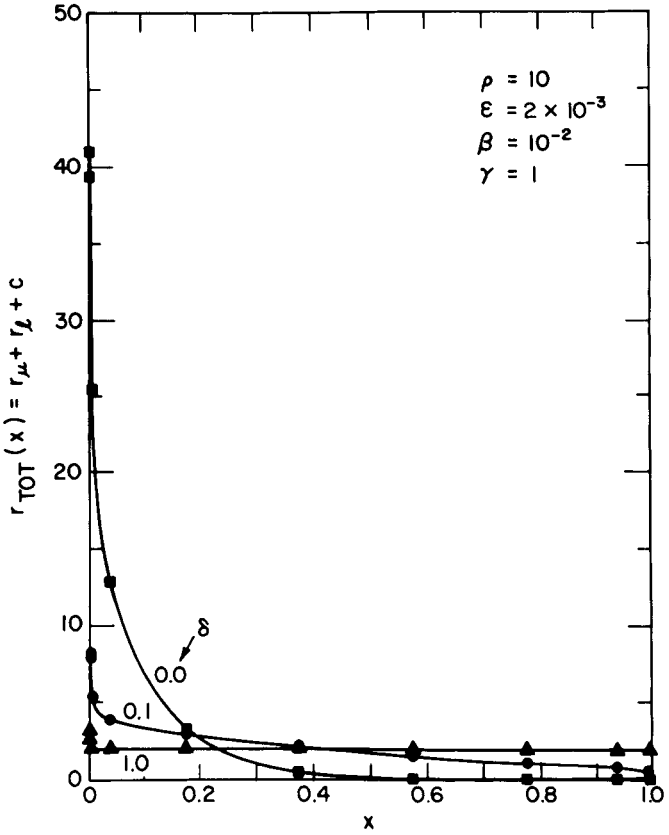


Fig. 10. Changes in receptor distribution as a cell goes from sliding motion ($\delta = 0$) to rolling motion ($\delta = 1$). Parameters other than $\delta$ are as shown in Table II.

It is difficult to see how the Thy-1 marker could be resorbed and inserted in a normal manner while retaining its labeling with fluoresceinated antibody. Thus, according to our analysis, Middleton's results are strong evidence against recirculating flow of the type proposed by Abercrombie et al [1972].

A treatment completely analogous to the derivation of Equation (28) shows that the recirculating flow model leads to a singularity in cell velocity at a critical value of the shear force. Thus, as with the sliding cell, there is a force at which the cell must begin to roll or be torn free of the surface.

## CONCLUSION

The most general conclusion resulting from our analysis of the reaction-convection hypothesis is that diffusion in cell membranes is too slow to counteract the effect of very mild convective currents with velocities on the order of one cell diameter per minute. This means that it is very reasonable to suppose that redistribution of receptors can be driven by convective flow. It also means that it is unreasonable to assume [Bretcher, 1976] that the relatively minor differences in diffusion constant between monomeric and polymeric receptors will have a controlling influence on whether or not redistribution occurs.

We have shown that redistribution can be caused by the relative motion of the cell and the surface or by a bottleneck in the recirculation of membrane. We have also shown

that cell rolling or excessive recirculation counteracts receptor redistribution. Quantitative observations of receptor redistribution can distinguish between various models of membrane flow (eg, rolling, sliding, recirculating). Such observations can also give information on the speed of the membrane flow, the diffusion constant of the receptors, and the rate constants for reaction between the receptors and the surface (ie, $k_+B_S$ and $k_-$).

Observations of the velocity of cells in the presence of fluid flow can give information on the strength of the adhesive attachments between the cell and the surface (ie, $\Omega'$) and give independent data on the other aspects of our model. Another conclusion of our analysis is that the recirculating flow hypothesis cannot account for the leading and trailing boundary layer structures observed by King et al [1980]. This is quite a general result, which argues strongly against models of the type advanced by Abercrombie et al [1972] and by Harris and Dunn [1972] and also those of the type advanced by Stossel [1977]. The presence of these boundary layer structures is also inconsistent with cell rolling. Of the models we have examined, the only one that gives a satisfactory explanation of the existing data is the simple sliding cell with negligible membrane flow and with negligible insertion and resorption of receptors. This tends to support the idea that receptors that are in close proximity while bound to the surface are analogous to cross-linked receptors and that such receptors are coupled to the force-generating apparatus of the cell by a mechanism similar to the mechanisms proposed by Bourguignon and Singer [1977] and Klausner et al [1980].

In light of this conclusion, our analysis of the reaction-convection hypothesis raises an interesting question concerning the mechanism of cell motion. Since the leading edge of a cell must apply traction to the surface in order for a cell to move, it is clear that a minimum density of certain types of receptors at the leading edge will be required for cell motion. However, we have shown that the sliding mode of motion will deplete the leading edge of adhesive receptors. How then does the sliding cell continue to move?

There can be several possible answers to this paradox. First, the cell may not move continuously, and diffusion could replenish the receptors at the leading edge if the cell paused or slowed down from time to time. Second, the number of receptors of the appropriate type may be present in great excess so that even if their numbers are reduced by 100- or 1,000-fold there will still be a sufficient supply to maintain cell motion. We know of no currently available data that can eliminate either of these possibilities.

## APPENDIX A. DERIVATION OF AN APPROXIMATE EXPRESSION FOR THE FLUX OF RECEPTORS PARALLEL TO THE y AXIS

In order to obtain an approximate expression for $\phi(x)$ in Equation (11) we note that unless the initial distributions of $\hat{r}_u$ and $\hat{r}_\ell$ are pathological, $\hat{r}_u$ and $\hat{r}_\ell$ will be symmetric about the x axis; and, consequently, $\partial_y \hat{r}_u = \partial_y \hat{r}_\ell = 0$ at $y = 0$. Furthermore, for physically realistic initial conditions, we expect $y = 0$ to be the only point at which the y components of the gradients of $\hat{r}_u$ and $\hat{r}_\ell$ vanish for all x between 0 and 1. In addition, it is clear that, since cell motion tends to remove receptors from the lower surface and add receptors to the upper surface, the extremum of $\hat{r}_u$ at $y = 0$ will be a maximum, whereas the extremum of $\hat{r}_\ell$ will be a relative minimum.

Since Equations (9a), (9b), and (9c) are linear and separable, an expression for $\hat{r}_u$ that is a solution to the equations and that has the desired properties can be constructed from a superposition of functions of the form

$$\hat{r}_u = G_u(x,\tau)\cos(k_u y). \tag{A1}$$

Similarly, $\hat{r}_\ell$ can be expressed as a sum of terms of the form

$$\hat{r}_\ell = G_\ell(x,\tau)\cosh(k_\ell y), \tag{A2}$$

where $k_u$ and $k_\ell$ are constants.

We now make the ansatz that $\hat{r}_u$ and $\hat{r}_\ell$ can be approximated by a single term of the appropriate form, but where $k_u$ and $k_\ell$ are allowed to be slowly varying functions of x and $\tau$. Under this presumption, we integrate Equations (A1) and (A2) with respect to y in order to express $G_u$ and $G_\ell$ in terms of $r_u$ and $r_\ell$, where

$$r_u \equiv \int_0^1 \hat{r}_u dy = G_u[\sin(k_u)/k_u] \tag{A3}$$

and

$$r_\ell \equiv \int_0^1 \hat{r}_\ell\, dy = G_\ell[\sinh(k_\ell)/k_\ell]. \tag{A4}$$

Inverting Equations (A3) and (A4), we obtain the following approximate expressions for $\hat{r}_u$ and $\hat{r}_\ell$:

$$\hat{r}_u \cong k_u r_u \cos(k_u y)/\sin(k_u) \tag{A5}$$

and

$$\hat{r}_\ell \cong k_\ell r_\ell \cosh(k_\ell y)/\sinh(k_\ell). \tag{A6}$$

We now require that $k_u$ and $k_\ell$ be chosen so as to satisfy the boundary conditions (6a) and (6d). This implies that

$$\tan(k_u) = \sqrt{u}\,\tanh[\sqrt{u}\,k_u] \tag{A7}$$

and

$$k_b = \sqrt{u}\,k_u \tag{A8}$$

where $u \equiv r_u/r_\ell$.

Exact solutions to Equations (A7) and (A8) cannot be obtained; however, an excellent approximate solution is

$$k_u \cong (\pi/2)[(u-1)/(u+1)]^{1/2} \tag{A9}$$

and

$$k_\ell \cong (\pi/2)[u(u-1)/(u+1)]^{1/2}. \tag{A10}$$

Table A1 shows a comparison of this approximate solution with exact numerical solutions

**TABLE AI. Comparison of Numerical and Approximate Analytic Solutions of Equation (A7)***

| $u = r_u/r_\ell$ | $k_u$ (numerical) | $k_u$ (approximate)* |
|---|---|---|
| 1 | 0 | 0 |
| 1.05 | 0.27 | 0.25 |
| 1.1 | 0.37 | 0.34 |
| 1.25 | 0.55 | 0.52 |
| 1.5 | 0.71 | 0.70 |
| 2.0 | 0.87 | 0.91 |
| 4.0 | 1.1 | 1.2 |
| 10.0 | 1.3 | 1.4 |
| $\infty$ | $\pi/2$ | $\pi/2$ |

*From Equation (A9).

of Equation (A7). As can be seen, the approximate solution is good to within 10% over the entire physical range of $1 \leqslant u \leqslant \infty$.

Finally, we see by differentiating Equation (A5) with respect to y that

$$\phi(x) \equiv (L^2/W^2)\partial_y r_u(x, 1) = -L^2 k_u^2 r_u/W^2.$$

If we now substitute Equation (A9) for $k_u$ we obtain

$$\phi(x) \cong \frac{-(\pi^2/4)L^2 r_u [r_u - r_\ell]}{W^2 [r_u + r_\ell]}. \tag{A11}$$

Since $r_u > r_\ell$ because redistribution removes receptors from the lower surface, we have that $0.5 \leqslant r_u/(r_u + r_\ell) \leqslant 1$. Thus, from Equation (A11) we obtain

$$\phi(x) \cong -[\omega^2 L^2/W^2][r_u - r_\ell], \tag{A12}$$

where $\omega^2 = 1.86 \pm 0.62$.

## APPENDIX B: APPROXIMATE SOLUTION TO A SPECIAL CASE OF THE MODEL BY MEANS OF BOUNDARY LAYER THEORY

The special case of Equations (11a–11c), applicable in the absence of cell rolling (ie, $\delta = 0$), and when the distributions of $r_u$, $r_\ell$, and c are time invariant (ie, $\partial_\tau r_u = \partial_\tau r_\ell = \partial_\tau c = 0$) is

$$0 = \epsilon\beta\partial_x^2 r_u - \rho^2\epsilon\beta(r_u - r_\ell) \tag{B1}$$

$$0 = \epsilon\beta\partial_x^2 r_\ell + \rho^2\epsilon\beta(r_u - r_\ell) - r_\ell + \gamma c \tag{B2}$$

and

$$0 = \beta\partial_x c + r_\ell - \gamma c. \tag{B3}$$

These equations are subject to the boundary conditions

$$r_\ell = r_u \text{ at } x = 0, 1 \tag{B4}$$

$$\epsilon\partial_x(r_\ell + r_u) + c = 0 \text{ at } x = 0, 1 \tag{B5}$$

$$c = 0 \text{ at } x = 1, \tag{B6}$$

and to the integral condition

$$\int_0^1 (r_u + r_\ell + c)dx = 2. \tag{B7}$$

Let us assume that $\tilde{r}_u$, $\tilde{r}_\ell$, and $\tilde{c}$ are solutions of Equations (B1–B6) but that these functions do not necessarily satisfy the integral condition (Equation B7). If we multiply Equations (B1–B6) by an arbitrary multiplicative constant, A, we see that the functions $A\tilde{r}_u$, $A\tilde{r}_\ell$, and $A\tilde{c}$ also satisfy Equations (B1–B6). Furthermore, if we choose

$$A = 2\left[\int_0^1 (\tilde{r}_u + \tilde{r}_\ell + \tilde{c})dx\right]^{-1} \tag{B8}$$

then $A\tilde{r}_u$, $A\tilde{r}_\ell$, and $A\tilde{c}$ will satisfy Equation (B7).

As a consequence of this property of the equations, we can proceed to solve Equations (B1–B6) subject to an arbitrary additional constraint and subsequently convert this solution into a solution of the full system by means of Equation (B8). We find that it is convenient to choose the condition

$$\tilde{r}_u(0) = 1 \tag{B9}$$

as the additional constraint that leads to the greatest simplification in the calculations.

If we add Equations (B1), (B2), and (B3), integrate between 0 and x, and apply the boundary condition (B5), we obtain

$$\tilde{c} = -\epsilon\partial_x(\tilde{r}_\ell + \tilde{r}_u) \quad 0 \leqslant x \leqslant 1. \tag{B10}$$

Substituting this expression for $\tilde{c}$ into Equations (B1) and (B2), we obtain

$$0 = \epsilon\beta\partial_x^2\tilde{r}_u - \rho^2\epsilon\beta(\tilde{r}_u - \tilde{r}_\ell) \tag{B11}$$

and

$$0 = \epsilon\beta\partial_x^2\tilde{r}_\ell - \epsilon\gamma\partial_x(\tilde{r}_\ell + \tilde{r}_u) + \rho^2\epsilon\beta[\tilde{r}_u - \tilde{r}_\ell] - \tilde{r}_\ell \tag{B12}$$

as coupled equations for $\tilde{r}_u$ and $\tilde{r}_\ell$. From Equations (B4), (B6), and (B9), we see that the

appropriate boundary conditions for (B11) and (B12) are:

$$\tilde{r}_\ell = \tilde{r}_u \text{ at } c = 0, 1 \tag{B13}$$

$$\tilde{r}_u(0) = 1 \tag{B14}$$

and

$$\partial_x(\tilde{r}_\ell + \tilde{r}_u) = 0 \text{ at } x = 1. \tag{B15}$$

On the basis of Equation (25) and numerical simulations, it appears that redistribution of receptors requires that $\epsilon\beta$, $\epsilon\gamma$, and $\epsilon$ are all $\ll 1$. However, since $\epsilon\beta$ multiplies a second derivative term in Equation (B12), whereas $\epsilon\gamma$ multiplies a first derivative term, it is convenient to define a new parameter $\alpha$ such that $\epsilon\beta = \alpha(\epsilon\gamma)^2$, ie,

$$\alpha \equiv \beta/\epsilon\gamma^2. \tag{B16}$$

In terms of $\alpha$ Equations (B11) and (B12) become

$$0 = (\epsilon\gamma)^2\partial_x^2\tilde{r}_u - \rho^2(\epsilon\gamma)^2(\tilde{r}_u - \tilde{r}_\ell) \tag{B17}$$

and

$$0 = \alpha(\epsilon\gamma)^2\partial_x^2\tilde{r}_\ell - (\epsilon\gamma)\partial_x(\tilde{r}_\ell + \tilde{r}_u) + \rho^2\alpha(\epsilon\gamma)^2[\tilde{r}_u - \tilde{r}_\ell] - \tilde{r}_\ell = 0. \tag{B18}$$

Since $\epsilon\gamma$ is small, we now expand $\tilde{r}_u$ and $\tilde{r}_\ell$ as power series in this parameter

$$\tilde{r}_u = U_0 + (\epsilon\gamma)U_1 + (\epsilon\gamma)^2U_2 + \cdots \tag{B19}$$

and

$$\tilde{r}_\ell = V_0 + (\epsilon\gamma)V_1 + (\epsilon\gamma)^2V_2 + \cdots. \tag{B20}$$

In order to obtain the approximate solutions for $\tilde{r}_u$ and $\tilde{r}_\ell$ valid in the interior, ie, away from the boundaries at $x = 0$ and 1, we substitute (B19) and (B20) into (B17) and (B18) and collect terms of $0(1)$ and of $0(\epsilon\gamma)$. The resulting equations for $U_0$, $V_0$, $U_1$ and $V_1$ are

$$\partial_x^2U_0 - \rho^2U_0 = 0$$

$$V_0 = 0$$

$$\partial_x^2U_1 - \rho^2U_1 + \rho^2V_1 = 0$$

and

$$-\partial_x(U_0 + V_0) - V_1 = 0.$$

These equations are readily solved with the result that

$$U_0 = K_1 \cosh(\rho x) + K_2 \sinh(\rho x) \tag{B21}$$

$$V_0 = 0 \tag{B22}$$

$$U_1 = (\rho^2 x/2)U_0 + K_3 \cosh(\rho x) + K_4 \sinh(\rho x) \tag{B23}$$

and

$$V_1 = -\partial_x U_0 = -\rho[K_1 \sinh(\rho x) + K_2 \cosh(\rho x)] \tag{B24}$$

where $K_1$, $K_2$, $K_3$, and $K_4$ are arbitrary constants yet to be specified.

In order to determine the behavior of the solution close to $x = 0$, we introduce the stretched variable

$$\zeta = x/\epsilon\gamma. \tag{B25}$$

In terms of $\zeta$, Equations (B17) and (B18) become

$$0 = \partial^2_\zeta \tilde{r}_u - \rho^2(\epsilon\gamma)^2(\tilde{r}_u - \tilde{r}_\ell) \tag{B26}$$

and

$$0 = \alpha\partial^2_\zeta \tilde{r}_\ell - \partial_\zeta(\tilde{r}_\ell + \tilde{r}_u) + \rho^2\alpha(\epsilon\gamma)^2[\tilde{r}_u - \tilde{r}_\ell] - \tilde{r}_\ell = 0. \tag{B27}$$

Near $x = 0$, we once again assume that $\tilde{r}_u$ and $\tilde{r}_\ell$ can be expanded as power series in $(\epsilon\gamma)$, $\tilde{r}_u = U_0' + (\epsilon\gamma)U_1' + (\epsilon\gamma)^2 U_2'$ and $\tilde{r}_\ell = V_0' + (\epsilon\gamma)V_1' + (\epsilon\gamma)^2 U_2'$, where primes are used to indicate that the various Us and Vs are regarded as functions of $\zeta$ rather than as functions of x. Substituting these expansions into Equations (B26) and (B27), collecting terms of $0(1)$ and $0(\epsilon\gamma)$, and solving the resulting equations for $U_0'$, $U_1'$, $V_0'$, and $V_1'$, we obtain

$$U_0' = J_1 + J_2\zeta,\ V_0' = J_3 \exp[\lambda_+\zeta] + J_4 \exp[\lambda_-\zeta] - J_2,\ U_1' = J_5 + J_6\zeta, \text{ and} \tag{B28}$$

$$V_1' = J_7 \exp[\lambda_+\zeta] + J_8 \exp[\lambda_-\zeta] - J_6,$$

where $J_1$–$J_8$ are arbitrary constants yet to be determined and

$$\lambda_\pm = (1/2\alpha)(1 \pm \sqrt{1 + 4\alpha}). \tag{B29}$$

In order to determine the Js, we first note that the limiting behavior of Equations (B28–B32) as $\zeta \to \infty$ must "match" with the limiting behavior of (B21–B24) as $x \to 0$. For example, if $x \to 0$, then

$$\tilde{r}_u \cong (U_0 + \epsilon\gamma U_1) = K_1 + \epsilon\gamma K_3 + K_2\rho x + (\epsilon\gamma\rho^2 K_2 x/2) + \epsilon\gamma K_4 \rho x + \cdots =$$

$$K_1 + \epsilon\gamma K_3 + \epsilon\gamma\rho K_2\zeta + 0[(\epsilon\gamma)^2];$$

whereas if $\zeta$ is large, $\tilde{r}_u \cong U_0' + \epsilon\gamma U_1' \cong J_1 + J_2\zeta + \epsilon\gamma J_5 + \epsilon\gamma J_6\zeta + 0[(\epsilon\gamma)^2]$.

Equating the coefficient of corresponding terms in these two representations of $\tilde{r}_u$, we conclude that

$$J_1 = K_1, J_2 = 0, J_5 = K_3 \text{ and } J_6 = \rho K_2. \tag{B30}$$

A similar matching procedure applied to the expressions for $\tilde{r}_\ell$ in the interior and near $x = 0$ yields the result that

$$J_3 = J_7 = 0 \tag{B31}$$

since these coefficients multiply terms which grow exponentially in the boundary layer.

In order to obtain more information on the unknown coefficients of Equation (B28) we apply the boundary conditions at $x = 0$ (B13 and B14) subject to the constraints of (B30) and (B31). This procedure leads to the result that

$$J_1 = 1, J_3 = 1, J_5 = 0, \text{ and } J_6 = \rho K_2. \tag{B32}$$

In light of (B30), (B31), and (B32), the solutions near $x = 1$ become

$$\tilde{r}_u = U_0' + \epsilon\gamma U_1' = 1 + \epsilon\gamma\rho K_2\zeta \tag{B33}$$

and

$$\tilde{r}_\ell \cong V_0' + \epsilon\gamma V_1' = \exp[\lambda_-\zeta] + \epsilon\gamma\rho K_2[\exp[\lambda_-\zeta - 1], \tag{B34}$$

whereas the solutions in the interior are

$$\tilde{r}_u \cong U_0 + \epsilon\gamma U_1 = \cosh(\rho x) + K_2 \sinh(\rho x) + \epsilon\gamma K_4 \sinh(\rho x) \tag{B35}$$

and

$$\tilde{r}_\ell \cong V_0 + \epsilon\gamma V_1 = \epsilon\gamma\rho[\sinh(\rho x) + K_2 \cosh(\rho x)]. \tag{B36}$$

To obtain the solution near $x = 1$, we introduce the stretched variable

$$\eta \equiv (x - 1)/(\epsilon\gamma) \tag{B37}$$

and proceed in a manner completely similar to that used to obtain the solution near $x = 0$. The initial expressions for the various terms in the series expansions of $\tilde{r}_\ell$ and $\tilde{r}_u$ near $x = 1$ are exactly the same as the corresponding terms near $x = 0$ (Equation B28), except that $\eta$ replaces $\zeta$. Nevertheless, the requirements of matching with the interior and of the boundary conditions are quite different for the two boundaries. We find that the solutions for $\tilde{r}_\ell$ and $\tilde{r}_u$ near $x = 1$ are*

$$\tilde{r}_u \cong [U_0'' + \epsilon\gamma U_1''] = \frac{\epsilon\gamma\rho}{\sinh(\rho)}\left[\frac{(1 + \lambda_+)}{\lambda_+} - \eta\right] \tag{B38}$$

*Note that double primes on the Us and Vs are used to indicate that the various terms in the series expansions of $\tilde{r}_\ell$ and $\tilde{r}_u$ near $x = 1$ are to be regarded as functions of $\eta$.

and

$$\tilde{r}_\ell = [V_0'' + \epsilon\gamma V_1''] = \frac{\epsilon\gamma\rho}{\sinh(\rho)}\,[1 + (1/\lambda_+)\exp(\lambda_+\eta)]. \tag{B39}$$

The matching conditions at x = 1 also imply that

$$K_2 = -\coth(\rho) \text{ and } K_4 = [\lambda_+ + 1]\rho/[\lambda_+ \sinh^2(\rho)] \tag{B40}$$

so that the remaining unknown coefficients of the expressions for $\tilde{r}_u$ and $\tilde{r}_\ell$ in the interior (ie, Equations B35 and B36) are determined.

Expressions for $\tilde{r}_\ell$ and $\tilde{r}_u$ which are uniformly valid in the interior, near x = 0 and near x = 1 are obtained by adding together the solutions appropriate for these three regions and subtracting from this sum those terms that are common to the interior and either of the boundaries. Thus, the uniform approximation to $\tilde{r}_\ell$ given in Equation (26b) is

$$\tilde{r}_\ell \cong (V_0 + \epsilon\gamma V_1) + (V_0' + \epsilon\gamma V_1') + (V_0'' + \epsilon\gamma V_1'') - (V_0' + \epsilon\gamma V_1')_{\xi\gg 1} -$$

$$(V_0'' + \epsilon\gamma V_1'')_{\eta\ll -1}.$$

Equation (26a) is the corresponding expression for $\tilde{r}_u$, whereas the expressions for A and $\tilde{c}$ in Equations (26e) and (26c) result from application of Equations (B8) and (B10), respectively.

## REFERENCES


Abercrombie, M., Heaysman, J.E.M., and Pegrum, S.M. (1972): Locomotion of fibroblasts in culture, V. Surface marking with concanavalin A. Exp. Cell Res. 73:536–539.

Armstrong, P.B. and Lackie, J.M. (1975): Studies on intercellular invasion in vitro using rabbit peritoneal neutrophil granulocytes (PMNs). J. Cell Biol. 65:439–462.

Atherton, A. and Born, G.V.R. (1972): Quantitative investigations of the adhesiveness of circulating polymorphonuclear leukocytes to blood vessel walls. J. Physiol. 222:447–485.

Bell, G.I. (1978): Models for specific adhesion of cells to cells. Science 200:618–627.

Bell, G.I. (1979): Theoretical models for the specific adhesion of cells to cells or to surfaces. In Proceedings of Conference on Models of Biological Growth and Spread, Heidelberg, West Germany, pp. 367–376.

Bourguignon, L.R.W. and Singer, S.J. (1977): Transmembrane interactions and the mechanism of capping of surface receptors by specific ligands. Proc. Natl. Acad. Sci. USA 74:5031–5035.

Bretcher, M.S. (1976): Directed lipid flow in cell membranes. Nature 260:21–23.

Cherry, R.J. (1979): Rotational and lateral diffusion of membrane proteins. Biochem. Biophys. Acta 559:289–327.

Elson, E.L., Schlessinger, J., Koppel, D.E., Axelrod, D., and Webb, W.W. (1976): Measurement of lateral transport on cell surfaces. In Marchesi, T. (ed.): "Membranes and Neoplasia." New York: A. R. Liss, Inc., pp. 137–149.

Gear, G.W. (1973): "Numerical Initial Value Problems in Ordinary Differential Equations." Englewood Cliffs, New Jersey: Prentice-Hall.

Greenwood, B. (1969): The motility of blood eosinophils on glass. Br. J. Derm. 81 (Suppl. 3):36–37.

Harris, A. and Dunn, G. (1972): Centripetal transport of attached particles on both surfaces of moving fibroblasts. Exp. Cell Res. 73:519–523.

Harris, A.K. (1973): Cell surface movements related to locomotion of tissue cells. Ciba Symp. 14:3–26.

Harris, A.K. (1976): Recycling of dissolved plasma membrane components as an explanation of capping. Nature 263:781–783.

King, C.A., Preston, T.M., Miller, R.H., and Donovan, P. (1980): Cell-substrate interactions during amoeboid locomotion of neutrophil leukocytes. Exp. Cell Res. 126:453–458.

Klausner, R.D., Bhalla, D.K., Dragsten, P, Hoover, R.L., and Karnovsky, M.J. (1980): Model for capping derived from inhibition of surface capping by free fatty acids. Proc. Natl. Acad. Sci. 77: 437–441.

Madras, P.N., Morton, W.A., and Petschek, H.E. (1971): Dynamics of thrombus formation. Fed. Proc. 30:1665–1667.

Middleton, C.A. (1979): Cell surface labeling reveals no evidence for membrane assembly and disassembly during fibroblast locomotion. Nature 282:203–205.

Ramsey, W.S. (1972a): Analysis of individual leukocyte behavior during chemotaxis. Exp. Cell Res. 70:129–139.

Ramsey, W.S. (1972b): Locomotion of human polymorphonuclear leukocytes. Exp. Cell Res. 72:489–501.

Robineaux, R. (1954): Mouvements cellulaires et fonction phagocytaire des granulocytes neutrophiles. Rev. Hematol. 9:364–402.

Ryan, G.B., Borysenko, J.Z., and Karnovsky, M.J. (1974): Factors affecting the redistribution of surface-bound concanavalin A on human polymorphonuclear leukocytes. J. Cell Biol. 62:351–365.

Senda, N., Tamura, H., Shibata, N., Yoshitake, J., Kondo, N., and Tanaka, K. (1975): The mechanism of movement of leukocytes. Exp. Cell Res. 91:393–407.

Stossel, T.P. (1977): Motile functions of phagocytic effector cells. In Cooper, M.D. and Dayton, D.H. (eds.): "Development of Host Defenses." New York: Raven Press, pp. 187–200.